ACS Photonics

Article

pubs.acs.org/journal/apchd5

Nanoscopic Study on Developing Optical Activity with Increasing Chirality for Two-Dimensional Metal Nanostructures

Tetsuya Narushima, Shun Hashiyada, and Hiromi Okamoto*

Institute for Molecular Science and The Graduate University for Advanced Studies (Sokendai), 38 Nishigonaka, Myodaiji, Okazaki, Aichi 444-8585, Japan

ABSTRACT: We studied the correlation between the geometry and the local optical activity of an "S"-shaped chiral nanostructure composed of two associating achiral "C"-shaped partial structures as one way to elucidate how optical activity develops with the formation of a chiral structure. This chirality formation process models the formation of chiral molecules by association of achiral atoms or functional groups. The local optical activities induced by the association of the achiral nanostructures were investigated using a circular dichroism (CD) nanoimaging technique. The chirality formed with the two approaching achiral partial structures caused enhancement of the local optical activity around the region of their connection when the distance between the achiral partial structures was less than 350 nm. The local optical activity was enhanced even without physical contact of the two partial structures. We therefore concluded that long-range electromagnetic interaction, rather than electronic exchange between the two partial structures, made a major contribution to the optical activity of the chiral nanostructure.

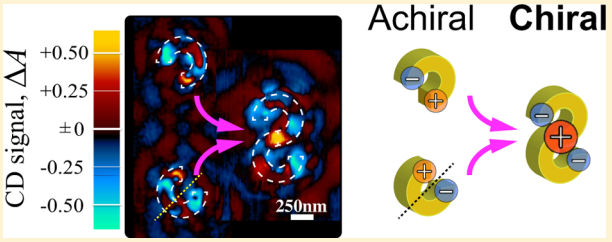

KEYWORDS: *chirality, optical activity, circular dichroism, nanostructure, scanning near-field optical microscope*

Chiral molecules, which have nonsuperimposable mirror images, show optical activity, such as optical rotation or circular dichroism (CD). A molecule composed of atoms (achiral) and/or functional groups (chiral or achiral) shows optical activity when the configuration of the atoms in the entire molecule is chiral.[1] Recently, optical activity caused not by molecular chirality but by chirality of nanostructured materials has been reported.[2,3] The nanostructures studied usually consisted of achiral atoms or molecules, and no compositional elements of the nanostructure had cause to be optically active. Instead, the optical activity of the nanostructure arises from a chiral geometry of the entire nanostructure.[4,5] How, then, does the light recognize the chiral geometry of the nanostructure that shows the optical activity? Optical interactions (absorption and scattering) in the nanostructures occur at each local area, and the local interactions integrated over the entire area of the nanostructure may correspond approximately to the total optical response of the system. To answer the question above, we must reveal the physical processes that cause the optical activity at the local areas and the influence of intersite interactions in the nanostructure.

The optical activity of some plasmonic nanostructures has been investigated based on theoretical analyses,[6,7] electromagnetic simulations,[5] and macroscopic measurements with propagating polarized light.[4,8−10] It was previously reported that various chiral geometries of the nanostructures, e.g., many types of planar chiral structures[2,4,6−8,10] as well as three-dimensional (3D) structures such as a helix,[9,11] showed optical activity.[3] On the basis of theoretical simulations for various nanostructures, it has been pointed out that some 3D metal nanostructures yield large chiroptical interaction.[5] Some pioneering works were reported to control the optical activity through electromagnetic coupling of nanostructures[12] or external stimuli via photoexcitation.[13] For a deeper understanding of the characteristics and origins of the optical activity in various nanostructures, an optical-activity-based microscopic imaging technique would be advantageous. This approach provides information on the local optical activity at each position of the nanostructures and its dependence on the shapes and the sizes. The microscopic approach has the potential to elucidate the critical part of the nanostructure that makes the essential contribution to the chiral interaction between light and matter. We recently developed a local CD nanoimaging technique based on a scanning near-field optical microscope (SNOM) as a direct experimental method to explore local optical activity. With this technique, we demonstrated the existence of prominent localized optical activity in the chiral nanostructures[14] and revealed the correlation between the macroscopic optical activity of the entire nanostructure and the local optical activity of the same material.[15]

In this work, as an approach to observe how the optical activity develops with the formation of a chiral structure, we investigated the correlation between the geometry and the local optical activity for the chiral nanostructure composed of two associating achiral partial structures. We prepared a series of gold nanostructures composed of two achiral "C"-shaped nanostructures approaching each other in a two-dimensional

Received: May 16, 2014
Published: July 18, 2014

(2D) plane to form a chiral "S"-shaped nanostructure, in a way similar to the assembly of achiral atoms or functional groups to form chiral molecules. Using a near-field CD nanoimaging technique, we observed the development of local CD signals associated with the two approaching achiral "C" structures to obtain chirality. The individual achiral "C" nanostructures did not show any macroscopic optical activity because of the lack of structural chirality. By visualizing the local CD signal development with the formation of the chiral structure from the achiral components, we obtained information on the electromagnetic interactions involved in the optical activity that was induced by the acquired structural chirality. Elucidating the electromagnetic mechanism of the optical activity generated through the formation of the chiral structure may lead to the design of spatial structures and the strength of chiral optical fields in nanomaterials.

RESULTS AND DISCUSSION

Figure 1 shows the macroscopic CD and extinction spectra of the arrayed achiral C-shaped and the chiral S-shaped nanostructures and a near-field CD image for a single C-shaped nanostructure. The CD spectrum of the C-shaped nanostructure array did not show any distinct signals over the entire range of the measured wavelengths, in contrast to the CD spectra of the S-shaped chiral nanostructure arrays, as shown in Figure 1a. This result is reasonable, considering that the C-shaped nanostructure is achiral, because the CD is defined as the differential absorbance of left and right circularly polarized light (LCP and RCP, respectively): $\Delta A = A_{LCP} - A_{RCP}$. Extinction spectra of the C-shaped and the S-shaped nanostructures are shown in Figure 1b. These extinction spectra for all the nanostructures showed broad bands in the region between 500 and 900 nm with peaks at 710 nm arising from the plasmonic resonance. Although the C-shaped nanostructures did not show CD activity, the extinction spectrum was very similar to those of the S-shaped nanostructures. In the near-field CD image in Figure 1c, both positive and negative CD signals were found locally in the individual C-shaped nanostructure. The CD signals with opposite signs were distributed antisymmetrically at both ends of the C-shaped nanostructure, similar to the north and south poles of a horseshoe magnet. The macroscopic and local measurements thus indicate that the nanostructures show local optical activity even if the structure is not chiral, whereas the whole achiral nanostructure is optically inactive macroscopically, which is consistent with theoretical predictions previously reported.[16,17] The spatial structure of the CD signal distribution in Figure 1c, which showed a positive CD signal at the starting point of "C" and a negative signal at the terminal point, correctly reflected the symmetry of the C-shaped structure with a plane of mirror symmetry. The nonuniform local CD signals suggest that optical activity of the nanostructure should relate to resonant plasmon-mode structure in addition to structural symmetry of the *entire* nanostructure. The absence of macroscopic optical activity of the entire achiral nanostructure can thus be understood as a consequence of counterbalancing between the positive and negative CD signals, which are distributed antisymmetrically in the single C-shaped structure.[15] Previously, U-shaped structures were investigated with the second harmonic generation (SHG)-CD microscopic technique.[18] The U-shaped structure, which is similar to the C-shaped structure, showed extrema of the SHG-CD signal at the ends. In ref 18 the local signal extrema were attributed to charge

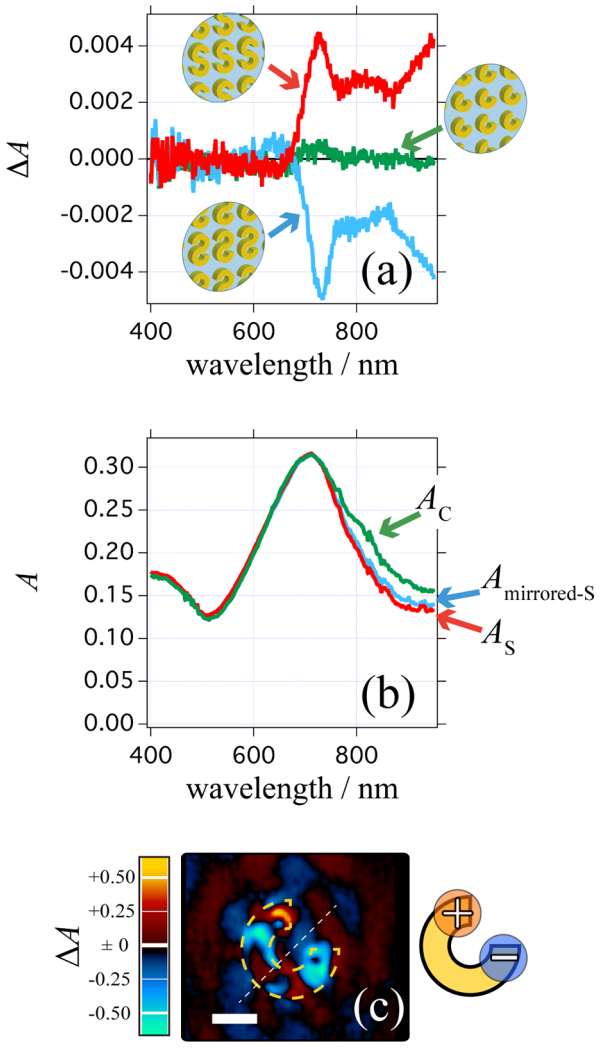

Figure 1. (a) Macroscopic CD spectra for C- and S-shaped gold nanostructures obtained using a conventional CD spectrometer. The arrayed samples of the achiral C-shaped and the chiral S-shaped nanostructures were used. Arrayed samples contained nanostructures rotated by every 30 degrees (0, 30, 60, ..., 330 degrees) to suppress commingling artifacts due to the orientation of the sample (linear dichroism).[15] The number density of the arrayed structures was 0.86 structure/μm^2. (b) Macroscopic extinction spectra for the C- and (mirrored) S-shaped nanostructures (A_C, A_S, and $A_{mirrored\text{-}S}$) measured under a standard far-field optical microscope. (c) Near-field CD image of an isolated C-shaped gold nanostructure observed at a wavelength of 785 nm. The scale bar represents 250 nm.

accumulation at the ends of these structures as a result of rotating charges in the nanostructure under LCP and RCP illuminations. The antisymmetric CD distribution observed for the C-shaped nanostructure in Figure 1c may be due to similar charge redistribution under circularly polarized light illumination, although quantitative analysis for resonant plasmon modes is necessary to investigate further details.

The two C-shaped nanostructures approaching each other formed the mirrored "S" structure, which enhanced the structural chirality of the entire system, as shown in Figure 2. Formation of the mirrored "S" structure was completed when the two starting points of the C-shaped structures, which showed positive CD signals, were linked together. We performed near-field CD imaging for the systems composed of the two C-shaped structures to observe the development of

dx.doi.org/10.1021/ph500171t | ACS Photonics 2014, 1, 732−738

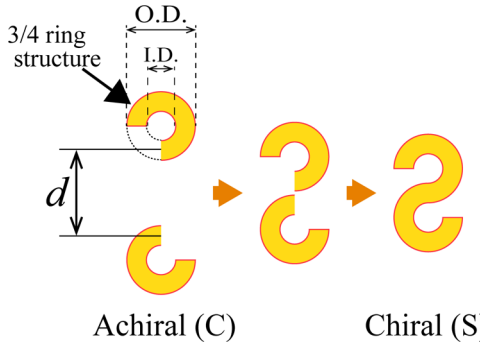

Figure 2. Formation of a chiral structure by association of achiral structures. The distance between two separated C-shaped nanostructures, *d*, is defined as illustrated. A chiral structure with a mirrored "S" structure is formed from two achiral C-shaped structures by reducing *d*.

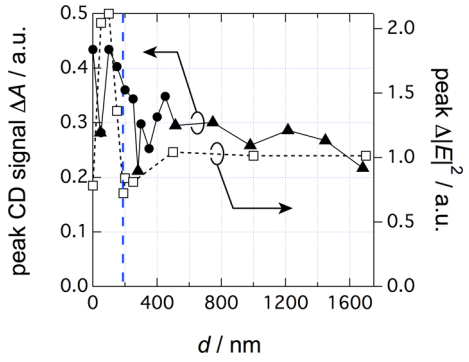

Figure 4. Local CD signal intensity near the connecting area as a function of the distance, *d*, between the C-shaped nanostructures. Peak values of the positive local CD signals near the connecting area, i.e., in the central region of the S-shaped structure, or regions of ≲300 nm from the starting points of "C" when *d* is large, were plotted with filled symbols. Filled circles represent CD signals obtained from the near-field CD images ($0 \leq d \leq 450$ nm) in Figure 2. Filled triangles are the plot for another set of samples that covers the larger *d* ($50 \leq d \leq 1680$ nm). The CD signal scales for two sets of measurements (short and long ranges in *d*) were corrected to give a smooth connection around $d \approx 400$ nm because the characteristics of the SNOM probes used for the short- and long-range samples were different, which caused a difference in the signals. The two C-shaped structures were in physical contact at $d \cong 190$ nm (indicated with the vertical dashed line). Open squares are the plot of peak values of $\Delta|E|^2$ evaluated from the electromagnetic simulation (Figure 5).

the CD signal with varying distances between the two partial structures. As shown in Figure 3, with decreasing distance *d* between the C-shaped nanostructures, positive CD signals at the central region of the system (corresponding to the starting points of the "C") showed a monotonic increase. The distance, *d*, was defined as shown in Figure 2. The positive CD signal in the central region was intensified with the reduction of the distance between the two achiral partial C-shaped structures, which enhanced the structural chirality. In contrast to the distinct change at the central region, no remarkable variation was observed for the CD distribution in the other areas. Small changes in the spatial distribution and intensities of the CD signals were recognized in the outer areas of the system. As discussed later, this minor change of the local CD distribution may contribute critically to the handedness of the macroscopic CD signal of the entire nanostructure.

To examine the detailed behavior of the CD at the central region, the change of positive CD signals (peak values of CD signals in the central region of the S-shaped structure, or regions where they are ≲300 nm from the starting points of "C" when *d* is large) is plotted in Figure 4 as a function of *d*. This figure involves the behavior of the CD signals for long distances, which was obtained from near-field CD images for samples with larger *d* ($50 \leq d \leq 1680$ nm), in addition to the near-field CD images in Figure 3 ($0 \leq d \leq 450$ nm). For $d \leq 350$ nm, the CD signal monotonically increased as *d* approached 0 to form the S-shaped structure. In contrast, for $d > 500$ nm, the CD signals at the starting points of the "C" were nearly constant. The peak value of the CD signal at $d = 0$, where the perfect S-shaped structure was formed, increased 1.5−2 times over the constant value observed for large *d*.

The individual C-shaped nanostructure has positive and negative CD signals at both ends, as shown in Figure 1c. The constant values of the CD signals observed for the long distances described above correspond to the positive local CD

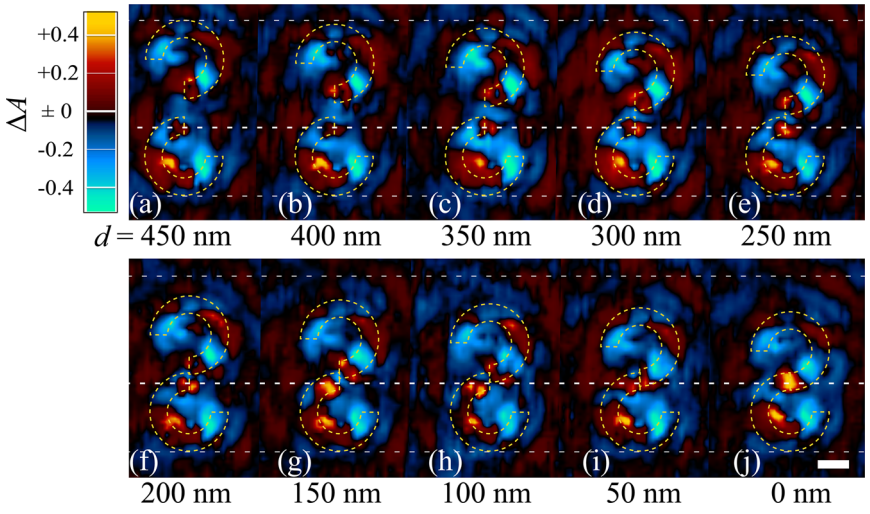

Figure 3. Near-field CD images of two C-shaped nanostructures approaching to form a mirrored S-shaped structure. The distance between the achiral C-shaped nanostructures (*d*) was varied from 450 to 0 nm by every 50 nm. The wavelength for the observation was 785 nm. The scale bar represents 300 nm.

dx.doi.org/10.1021/ph500171t | ACS Photonics 2014, 1, 732−738

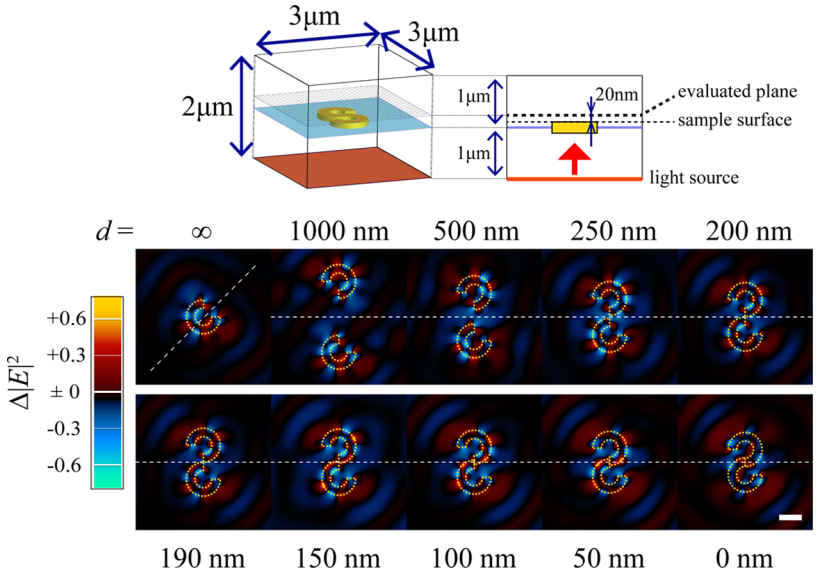

Figure 5. (Top) Configuration of the sample and the light source for the FDTD simulation. (Bottom) Spatial distributions of differential electric field intensities between the LCP and RCP illuminations, simulated with the FDTD method, for two approaching C-shaped gold nanostructures. The differential electric field intensities at each position were evaluated as $\Delta|E|^2 \equiv |E_{LCP}(x, y)|^2 - |E_{RCP}(x, y)|^2$. The intensity distribution at $d = \infty$ corresponds to an isolated C-shaped nanostructure. The wavelength of the excitation was 785 nm. The scale bar represents 500 nm.

that the C-shaped nanostructure originally had at its starting point of "C". In contrast, the increase of the CD signal seen at $d \leq 350$ nm was induced by the enhanced structural chirality of the system. With electron microscopy, the metallic parts of the C-shaped nanostructures were confirmed to be separated from each other at $d \geq 200$ nm. This observation indicates that the increase of the CD signals observed with decreasing d, especially at 350 nm $\geq d \geq$ 200 nm, may be attributed to long-range through-space interaction between the two C-shaped nanostructures and is not due to interexchange of conductive electrons in the metallic parts. At $d <$ 200 nm, where the metallic parts are in physical contact, no remarkable change in the slope of the CD signal increase was seen in comparison with the slope at $d \gtrsim 200$ nm. These experimental results suggest that the increase of the optical activity is not influenced very much by the physical contact of the metallic parts.

The phenomenon of the CD signal enhancement for associating partial nanostructures is seemingly similar to optical-field enhancements in nanoparticle assemblies.[19,20] The enhanced optical field is generated in the interstitial site when a nanoparticle assembly is irradiated with light. Highly enhanced optical fields, as high as 10^5 to 10^7 times in intensity ($\propto|E|^2$), are potentially generated because of induced electric charges with opposite signs at each surface of the interstitial sites between the proximally positioned nanoparticles. The remarkable enhancement of the optical field is observed only when the gap distance between the nanoparticles is less than 10 nm, although weaker enhancement occurs at larger distances of several tens to hundreds of nanometers. Enhancement of optical activity in the assembly of C-shaped structures was only up to a few times and only in the long-distance range, as is similar to the long-range field enhancement near a metal particle.[21] The mechanism of the local optical activity enhancement discussed here must therefore be different from that of the enormously enhanced fields in the gaps between nanoparticles.

The physical mechanisms of different optical responses to LCP and RCP illuminations in 2D chiral nanostructures were qualitatively discussed in the previous studies. The optical activities in 2D systems were attributed to dielectric losses[6,7] and characteristic behavior of rotating polarization induced by circularly polarized light.[14] These qualitative interpretations, however, are insufficient to discuss the magnitude of the optical activity and its shape dependence. Theoretical analyses incorporating the whole system of the measurement interacting with light, including the SNOM probe and the substrate, are necessary for detailed discussion in the future. This will lead us to a quantitative interpretation of the optical activity induced by the association of achiral nanostructures and the origin of the long-range ($d \approx 350$ nm) interaction between the partial structures that causes enhancement of the local optical activity. In the present study, to gain physical insights into the optical activity, we performed electromagnetic simulations on a simple model consisting only of nanostructures under far-field illumination with circularly polarized light, based on the finite-difference time-domain (FDTD) method. Because the focal spot size of the illumination in the imaging experiment was approximately 2.5 μm, we may consider that the two associated C-shaped nanostructures were nearly uniformly illuminated by the light in the sample we measured ($d \leq 1680$ nm). In the simulation, the entire structure was thus excited by a circularly polarized plane wave at a wavelength of 785 nm. The gold nanostructure with the same dimensions as the experiments was placed in an $x-y$ plane in the computational domain of $3 \times 3 \times 2$ μm^3. The electric field intensity ($|E|^2$) was evaluated at a plane 20 nm away from the sample surface in the direction of the propagation of the light to mimic the separation between the sample and the SNOM probe. The difference between $|E|^2$ for LCP illumination and $|E|^2$ for RCP illumination, $\Delta|E|^2$, was calculated for comparison with measured CD signals (ΔA) shown in Figure 3. The results are summarized in Figure 5. For the isolated C-shaped nanostructure (corresponding to $d = \infty$), a perfectly antisymmetric spatial distribution of $\Delta|E|^2$ with respect to the

dx.doi.org/10.1021/ph500171t | ACS Photonics 2014, 1, 732−738

plane of mirror symmetry was obtained. For dimeric structures of "C", the symmetric feature of individual "C" remained unchanged when the distance between the two was sufficiently large ($d \geq 1000$ nm). For shorter distances ($d \leq 500$ nm), the distribution of $\Delta|E|^2$ was remarkably changed, especially around the connection region (corresponding to the central region of "S"), and the symmetric feature of the individual "C" was diminished. The change became more distinct when the two C-shaped partial structures had physical contact ($d \leq 150$ nm). We should note that the simulation of $\Delta|E|^2$ did not directly model the experimental local CD observation because the observing system (the SNOM probe, in particular) was not considered in the simulation. However, we have found that the simulated $\Delta|E|^2$ in Figure 5 reproduces the qualitative feature of the observed CD images (Figure 3) for its localized positive $\Delta|E|^2$ values in the central region. The simulation also reproduced the overall spatial distributions of positive and negative signals in the entire nanostructure, although the peak values were not simulated accurately. For further detailed analysis, the observation system should be incorporated in the theoretical model, although it will be quite demanding work. Compared with the remarkable change in the central area of the structure, the peripheral region did not show noticeable change except for the completely connected case ($d = 0$).

Peak values of $\Delta|E|^2$ in the connecting area were evaluated and are plotted against the right axis in Figure 4 (open symbols), showing a prominent increase in the region $d \lesssim 200$ nm. The increased peak value of $\Delta|E|^2$ was approximately twice as large as the peak value of $\Delta|E|^2$ at a larger distance, which is comparable to the experimentally obtained result. The simulation reproduced the experimentally observed behavior of the CD signal on the whole, while the distance that showed the prominent increase of $\Delta|E|^2$ ($d \approx 200$ nm) was smaller than the distance obtained experimentally ($d \approx 350$ nm). Although we experimentally found a long-range interaction between the partial structures that gives rise to the enhanced CD signal, the simulation gave enhanced $\Delta|E|^2$ only when the two partial structures were in physical contact. The simulated results show a decrease in $\Delta|E|^2$, rather than an increase, in the region of $d =$ 300−200 nm, where the partial structures are separated. Further theoretical model analyses are necessary to clarify the origins of the long-range interaction that causes the CD enhancement. Another point that was not consistent with the experimentally measured behavior was that the peak value of $\Delta|E|^2$ suddenly decreased at $d = 0$ nm in the simulation. The origin of this behavior is also not clear at present.

We now analyze the signs of the CD signals. Both the near-field CD imaging and the FDTD simulation showed positive values of local CD signals and $\Delta|E|^2$ around the central region of the mirrored S-shaped structure. In contrast, as shown in Figure 1a, the macroscopic CD measurement for the entire nanostructure of the mirrored "S" exhibited a negative CD signal at the wavelength used for the near-field CD imaging (785 nm). As shown in Figure 1c, the individual C-shaped nanostructure showed positive and negative CD extrema at the starting and the terminal points, respectively. When the mirrored "S" is formed by connecting the two starting points of "C", the two positive CD maxima at the starting point of the "C" structures are merged to yield *one* positive maximum, while the *two* negative extrema at the terminal points remain. The merging of the positive CD maxima may thus provide a simple qualitative explanation for the negative CD dominating in the entire mirrored "S" nanostructures. However, the CD signal of the entire nanostructure depends on the local CD signal integrated over the entire structure. The detailed structure of the local CD distribution and magnitude must depend on the distance between the two C-shaped nanostructures. We therefore evaluated the integrated values over the entire nanostructure for the CD signals obtained by the near-field CD measurement and for the simulated $\Delta|E|^2$ values. In either case, the integrated value was negative, in contrast to the positive local CD signal and $\Delta|E|^2$ at the central region of the mirrored "S" structure, as is consistent with the simple consideration mentioned above. The local values at the center are inverted from the integrated values. This inverted relation suggests that minor changes in periphery, although they appeared to be negligibly small, made an important contribution to the optical activity integrated over the entire nanostructure. Our previous study of the S-shaped gold nanostructure showed that the local optical activity was 2 orders of magnitude larger than the macroscopic optical activity, and the integrated local optical activity agreed roughly with the macroscopically measured optical activity.[15] The present result also indicates that the optical activity of the entire system is influenced by the delicate balance of the spatial distribution of the local optical activity, in addition to the symmetry of the material, rather than by the local optical activity at a specific segment.

CONCLUSIONS

In this work, we studied the correlation between the geometry and the local optical activity for the chiral S-shaped nanostructure composed of two associating achiral C-shaped partial structures and discussed how optical activity develops with increasing structural chirality. Local optical activity of the achiral C-shaped nanostructure was visualized, while this nanostructure did not show any inherent macroscopic optical activity. The spatial distribution of the local CD signal reflected the symmetry of the C-shaped structure, possessing a plane of mirror symmetry. When a chiral mirrored "S" nanostructure was formed by two approaching C-shaped structures, positive CD signals around the connection region (corresponding to the central region of the system) showed a monotonic increase at $d \leq 350$ nm. The increase of the CD signal was induced by the enhanced structural chirality of the entire system. The metallic parts of the two C-shaped nanostructures were not in physical contact at $d \approx 350$ nm, where the CD signal began to increase. It was therefore suggested that the optical activity observed around the connection region was not caused by an interexchange of conductive electrons in the metallic parts but should be attributed to long-range electromagnetic interaction between the two C-shaped nanostructures. In the present near-field CD measurements, sufficient reproducibility of the CD signal intensity (variation ∼5% or less) was realized to discuss the monotonic increase of the CD signal reported in this article, as far as the same SNOM probe and the same nanostructure sample were used. In addition to the roughly monotonic behavior, rapid changes of the CD signal were observed at a couple of points in the short-distance region. To examine the reproducibility of these features, fabrication of nanostructures with finer d increments and measurements for the samples are necessary. Detailed analysis for the d-dependent behavior in this way may provide additional information on the chiral interaction between the partial structures in the future. Very recently, a relevant experimental study on nonlinear optical activity measurements for tuned chiral structures was

dx.doi.org/10.1021/ph500171t | ACS Photonics 2014, 1, 732−738

reported.[22] Contrary to our finding of the monotonic increase of the CD signal with enhanced structural chirality, they showed a local maximum of the signal at a certain value of the chiral structure parameter.

The present study demonstrated enhancement of (local) optical activity accompanied by increasing structural chirality based on direct microscopic measurements of the local CD. Full control of the optical activity of the materials may provide technological innovation relevant to the application of chiral materials. Some proposals[16] and demonstrations[23,24] have been reported, for example, on the application of chiral optical fields in the proximity of metal nanostructures to chemical analysis of chiral molecules. Toward this goal, it is crucial to clarify the plasmonic modes and the chiral electromagnetic interactions mediated in the nanostructure, which contribute to the enhancement of the optical activity. The controlled association of achiral nanostructures presented in this study can be one of the potential techniques to design local optical activity. An effective distance to induce optical activity was estimated to be ~350 nm in the system presently examined. The long-range interaction will provide a fine regulation of the optical activity by tuning the distance between nanostructures, and this principle may promote utilization of chiral interactions between the designed optically active materials and the molecules/materials nearby.

METHODS

Nanostructured Sample. In this study, 2D gold nanostructures were investigated. The nanostructures were fabricated on a glass substrate by the electron-beam lithography lift-off technique. The 2D chiral nanostructure with the "S" shape[14,15] was chosen to generate optical activity. The S-shaped structure is chiral in the 2D plane; that is, it is not superimposable on its mirror image. Two C-shaped structures, corresponding to a three-fourths segment of a ring, are obtained by dividing the S-shaped structure at the center. The divided C-shaped structure does not possess chirality (i.e., is achiral), which means that the mirrored image of the C-shaped structure is identical with the original structure. In an opposite way, the S-shaped structure is formed when two C-shaped structures are approaching, as shown in Figure 2. We performed near-field CD imaging measurements (described below) for the nanostructures composed of two C-shaped structures approaching each other. The measured values of the outer and inner diameters of the fabricated C-shaped nanostructure were 750 and 375 nm, respectively. The height of the S-shaped nanostructure was approximately 1300 nm. Gold films with a thickness of 35 nm were formed for the nanostructures by vacuum deposition onto an underlying 2-nm-thick chromium adhesion layer.

Near-Field CD Nanoimaging. To visualize the distribution of the local CD signals for the individual nanostructures, we incorporated a polarization modulation method using a photoelastic modulator, which is an established method in conventional CD spectrometers,[25] in a home-built collection-mode aperture-type scanning near-field optical microscope.[14] In the near-field CD nanoimaging, the entire nanostructured samples were excited by the light (far-field) through an objective lens (NA = 0.45). The measured diameter of the focused spot was approximately 2.5 μm. The local transmitted intensity (including both far-field and near-field components) through the sample structures was collected at each sample position by the aperture of the SNOM probe and then converted to the local CD signal through lock-in detection. The aperture diameter of the SNOM probes was typically 100 nm. The spatial resolution for the near-field CD imaging is given approximately by the aperture diameter.

We adopted $\Delta A = A_{LCP} - A_{RCP}$ as the definition of the CD signal, where A_{LCP} and A_{RCP} denote the absorbance of LCP and RCP, respectively. From the definition, $\Delta A > 0$ when the extinction for LCP is higher than the extinction for RCP. The quantity ΔA can be converted to the ellipticity θ, which is frequently used for the CD measurements of molecules, with the relation θ [deg] = 32.982ΔA when ΔA is sufficiently small.[1]

AUTHOR INFORMATION

Corresponding Author

*E-mail: aho@ims.ac.jp. Fax: +81-564-54-2254. Tel: +81-564-55-7320.

Notes

The authors declare no competing financial interest.

ACKNOWLEDGMENTS

The authors thank Ms. A. Ishikawa (IMS) for nanostructured sample fabrication and Mr. S. Makita (IMS) for his assistance in macroscopic CD measurements. This work was supported by Grants-in-Aid for Scientific Research (Grant Nos. 21655008, 22225002, 23760038, and 26410027) from the Japan Society for the Promotion of Science (JSPS), the Photon Frontier Network Program of the Ministry of Education, Culture, Sports, Science, and Technology (MEXT), Japan. T.N. is also grateful for the support given by the Research Foundation for Opto-Science and Technology, Japan.

REFERENCES

(1) Berova, N.; Nakanishi, K.; Woody, R. W. *Circular Dichroism: Principles and Applications*, 2nd ed.; Wiley-VCH: New York, 2000.

(2) Vallius, T.; Jefimovs, K.; Turunen, J.; Vahimaa, P.; Svirko, Y. Optical activity in subwavelength-period arrays of chiral metallic particles. *Appl. Phys. Lett.* **2003**, *83*, 234−236.

(3) Valev, V. K.; Baumberg, J. J.; Sibilia, C.; Verbiest, T. Chirality and chiroptical effects in plasmonic nanostructures: fundamentals, recent progress, and outlook. *Adv. Mater.* **2013**, *25*, 2517−2534.

(4) Kuwata-Gonokami, M.; Saito, N.; Ino, Y.; Kauranen, M.; Jefimovs, K.; Vallius, T.; Turunen, J.; Svirko, Y. Giant optical activity in quasi-two-dimensional planar nanostructures. *Phys. Rev. Lett.* **2005**, *95*, 227401-1−227401-4.

(5) Schäferling, M.; Dregely, D.; Hentschel, M.; Giessen, H. Tailoring enhanced optical chirality: design principles for chiral plasmonic nanostructures. *Phys. Rev. X* **2012**, *2*, 031010-1−031010-9.

(6) Fedotov, V. A.; Mladyonov, P. L.; Prosvirnin, S. L.; Rogacheva, A. V.; Chen, Y.; Zheludev, N. I. Asymmetric propagation of electromagnetic waves through a planar chiral structure. *Phys. Rev. Lett.* **2006**, *97*, 167401−167401−4.

(7) Fedotov, V. A.; Schwanecke, A. S.; Zheludev, N. I.; Khardikov, V. V.; Prosvirnin, S. L. Asymmetric transmission of light and enantiomerically sensitive plasmon resonance in planar chiral nanostructures. *Nano Lett.* **2007**, *7*, 1996−1999.

(8) Hendry, E.; Carpy, T.; Johnston, J.; Popland, M.; Mikhaylovskiy, R. V.; Lapthorn, A. J.; Kelly, S. M.; Barron, L. D.; Gadegaard, N.; Kadodwala, M. Ultrasensitive detection and characterization of biomolecules using superchiral fields. *Nat. Nanotechnol.* **2010**, *5*, 783−787.

(9) Hentschel, M.; Schäferling, M.; Metzger, B.; Giessen, H. Plasmonic diastereomers: adding up chiral centers. *Nano Lett.* **2013**, *13*, 600−606.

(10) Valev, V. K. Characterization of nanostructured plasmonic surfaces with second harmonic generation. *Langmuir* **2012**, *28*, 15454−15471.
(11) Gansel, J. K.; Thiel, M.; Rill, M. S.; Decker, M.; Bade, K.; Saile, V.; von Freymann, G.; Linden, S.; Wegener, M. Gold helix photonic metamaterial as broadband circular polarizer. *Science* **2009**, *325*, 1513−1515.
(12) Plum, E.; Fedotov, V. A.; Schwanecke, A. S.; Zheludev, N. I.; Chen, Y. Giant optical gyrotropy due to electromagnetic coupling. *Appl. Phys. Lett.* **2007**, *90*, 223113-1−223113-3.
(13) Lv, T. T.; Zhu, Z.; Shi, J. H.; Guan, C. Y.; Wang, Z. P.; Cui, T. J. Optically controlled background-free terahertz switching in chiral metamaterial. *Opt. Lett.* **2014**, *39*, 3066−3069.
(14) Narushima, T.; Okamoto, H. Circular dichroism nano-imaging of two-dimensional chiral metal nanostructures. *Phys. Chem. Chem. Phys.* **2013**, *15*, 13805−13809.
(15) Narushima, T.; Okamoto, H. Strong nanoscale optical activity localized in two-dimensional chiral metal nanostructures. *J. Phys. Chem. C* **2013**, *117*, 23964−23969.
(16) Schäferling, M.; Yin, X.; Giessen, H. Formation of chiral fields in a symmetric environment. *Opt. Express* **2012**, *20*, 26326−26336.
(17) Valev, V. K.; De Clercq, B.; Biris, C. G.; Zheng, X.; Vandendriessche, S.; Hojeij, M.; Denkova, D.; Jeyaram, Y.; Panoiu, N. C.; Ekinci, Y.; Silhanek, A. V.; Volskiy, V.; Vandenbosch, G. A. E.; Ameloot, M.; Moshchalkov, V. V.; Verbiest, T. Distributing the optical near-field for efficient field-enhancements in nanostructures. *Adv. Mater.* **2012**, *24*, OP208−OP215.
(18) Valev, V. K.; Silhanek, A. V.; De Clercq, B.; Gillijns, W.; Jeyaram, Y.; Zheng, X.; Volskiy, V.; Aktsipetrov, O. A.; Vandenbosch, G. A. E.; Ameloot, M.; Moshchalkov, V. V.; Verbiest, T. U-Shaped switches for optical information processing at the nanoscale. *Small* **2011**, *7*, 2573−2576.
(19) Okamoto, H.; Imura, K. Visualizing the optical field structures in metal nanostructures. *J. Phys. Chem. Lett.* **2013**, *4*, 2230−2241.
(20) Xu, H.; Aizpurua, J.; Käll, M.; Apell, P. Electromagnetic contributions to single-molecule sensitivity in surface-enhanced Raman scattering. *Phys. Rev. E* **2000**, *62*, 4318−4324.
(21) Novotny, L.; Hecht, B. *Principles of Nano-Optics*, 1st ed.; Cambridge University Press: Cambridge, 2006; pp 261−265.
(22) Valev, V. K.; Baumberg, J. J.; De Clercq, B.; Braz, N.; Zheng, X.; Osley, E. J.; Vandendriessche, S.; Hojeij, M.; Blejean, C.; Mertens, J.; Biris, C. G.; Volskiy, V.; Ameloot, M.; Ekinci, Y.; Vandenbosch, G. A. E.; Warburton, P. A.; Moshchalkov, V. V.; Panoiu, N. C.; Verbiest, T. Nonlinear superchiral meta-surfaces: tuning chirality and disentangling non-reciprocity at the nanoscale. *Adv. Mater.* **2014**, *26*, 4074−4081.
(23) Meinzer, N.; Hendry, E.; Barnes, W. L. Probing the chiral nature of electromagnetic fields surrounding plasmonic nanostructures. *Phys. Rev. B* **2013**, *88*, 041407-1−041407-5.
(24) Ma, W.; Kuang, H.; Xu, L.; Ding, L.; Xu, C.; Wang, L.; Kotov, N. A. Attomolar DNA detection with chiral nanorod assemblies. *Nat. Commun.* **2013**, *4*, 2689-1−2689-8.
(25) Drake, A. F. Polarisation modulation-the measurement of linear and circular dichroism. *J. Phys. E: Sci. Instrum.* **1986**, *19*, 170−181.